DALTON

Cluster core geometrical variation in heterometallic boride clusters containing $RhRu_4$ skeletons: crystal structures of $[RhRu_4H_2(\eta^5\text{-}C_5Me_5)(\mu\text{-}Cl)(CO)_{12}B]$ and $[RhRu_4H(nbd)(CO)_{12}B(AuPPh_3)]$ (nbd = norbornadiene)*

Andrew D. Hattersley,[a] Catherine E. Housecroft[b] and Arnold L. Rheingold[c]

[a] *University Chemical Laboratory, Lensfield Road, Cambridge CB1 2EW, UK*
[b] *Institut für Anorganische Chemie, Spitalstrasse 51, CH-4056, Basel, Switzerland*
[c] *Department of Chemistry, University of Delaware, Newark, DE 19 716, USA*

The reaction of the butterfly anion $[Ru_4H(CO)_{12}BH]^-$ with $[\{Rh(\eta^5\text{-}C_5Me_5)Cl_2\}_2]$ gave the novel boron-containing cluster $[RhRu_4H_2(\eta^5\text{-}C_5Me_5)(\mu\text{-}Cl)(CO)_{12}B]$ which has been characterised spectroscopically and by X-ray crystallography. Consistent with the 78 valence-electron (v.e.) count, the five metal atoms adopt an open skeletal structure which can be described as an 'envelope' (or an edge-bridged square) geometry. In contrast, when $[Ru_4H(CO)_{12}BH]^-$ reacted with $[\{Rh(nbd)Cl\}_2]$ (nbd = norbornadiene) and $[Au(PR_3)Cl]$ (R = Ph, C_6H_{11} or 2-MeC_6H_4), boride clusters containing both $RhRu_4B$ and Rh_2Ru_4B skeletons were obtained. The presence of the gold(I) phosphine is necessary to trap the $RhRu_4B$-containing product. The Rh_2Ru_4B clusters possess octahedral frameworks and are related to the previously reported $[Rh_2Ru_4(CO)_{16}B(AuPR_3)]$ compounds. However, the incorporation of only one rhodium fragment leads to the clusters $[RhRu_4H(nbd)(CO)_{12}B(AuPR_3)]$, and a square-based pyramidal $RhRu_4$ framework (consistent with a 74 v.e. count) has been confirmed by the results of a single-crystal X-ray diffraction study of $[RhRu_4H(nbd)(CO)_{12}B(AuPPh_3)]$. Variable-temperature ^1H NMR spectroscopic data for the clusters $[RhRu_4H(nbd)(CO)_{12}B(AuPR_3)]$ (R = Ph, C_6H_{11} or 2-MeC_6H_4) indicate fluxional behaviour involving the norbornadiene ligand and the gold(I) phosphine unit. The reaction of $[RhRu_4H(nbd)(CO)_{12}B(AuPR_3)]$ (R = Ph or C_6H_{11}) with CO gave $[RhRu_4H(CO)_{14}B(AuPR_3)]$.

Over the past few years the number of transition-metal clusters containing boron in interstitial and semi-interstitial environments has increased,[1,2] but there remains only a small number in which the boron is directly bonded to five metal atoms. An ambiguity immediately arises since a number of the borides prepared to date incorporate gold(I) centres in the metal framework. Commonly applied electron-counting schemes and discussions of cluster bonding do not place the gold(I) centre [which is present within a gold(I) phosphine fragment or as an isolated metal atom fusing together two sub-clusters] in a skeletal vertex site. For example, in the anion $[\{Ru_4H(CO)_{12}BH\}_2Au]^-$,[3] each boron atom is bonded to four skeletal ruthenium atoms and one (non-skeletal) gold atom. Similarly in $[Ru_5(CO)_{15}B(AuPPh_3)]$[4] [Fig. 1(*a*)] we would consider the boron atom to be in a semi-interstitial environment with respect to the pentaruthenium cage with a secondary interaction to a peripheral $AuPPh_3$ unit. Taken as such, the latter compound may be claimed to be the first pentametallic boride cluster but the claim is undoubtedly ambiguous. A true member of this group of clusters is $[Os_5H(CO)_{16}B]$ [Fig. 1(*b*)], prepared and structurally characterised by Shore and co-workers.[5] A further example is $[Co_5(CO)_{14}B(BH)]$ [Fig. 1(*c*)] but the close proximity of the two boron centres [1.85(4) Å] adds a different dimension of ambiguity to the structural description.[6]

In this paper we describe routes to heterometallic clusters, each of which contains an interstitial boron atom bonded to five d-block metals from Group 8 or 9.

Experimental

General data

Fourier-transform NMR spectra were recorded on a Bruker WM 250 or AM 400 spectrometer. The ^1H shifts are reported with respect to δ 0 for $SiMe_4$, ^{11}B with respect to δ 0 for $F_3B{\cdot}OEt_2$ and ^{31}P with respect to δ 0 for H_3PO_4. All downfield chemical shifts are positive. Infrared spectra were recorded on a Perkin-Elmer FT 1710 spectrophotometer, FAB (fast atom bombardment) mass spectra on Kratos instruments with a 3-nitrobenzyl alcohol matrix.

All reactions were carried out under argon using standard Schlenk techniques. Solvents were dried over suitable reagents and freshly distilled under N_2 before use. Separations were carried out by thin-layer plate chromatography with Kieselgel 60-PF-254 (Merck). The compounds $[\{Rh(nbd)Cl\}_2]$ (nbd = norbornadiene = bicyclo[2.2.1]hepta-2,5-diene), $[\{Rh(\eta^5\text{-}C_5Me_5)Cl_2\}_2]$ and $[\{Ir(\eta^5\text{-}C_5Me_5)Cl_2\}_2]$ were used as received (Aldrich); $[N(PPh_3)_2][Ru_4H(CO)_{12}BH]$[8] and $[Au(PR_3)Cl]$ (R = Ph, C_6H_{11} or 2-MeC_6H_4)[9] were prepared according to literature methods. Yields are quoted with respect to $[N(PPh_3)_2][Ru_4H(CO)_{12}BH]$.

Preparation of $[RhRu_4H_2(\eta^5\text{-}C_5Me_5)(\mu\text{-}Cl)(CO)_{12}B]$ 1

The dimer $[\{Rh(\eta^5\text{-}C_5Me_5)Cl_2\}_2]$ (30 mg, 0.05 mmol) was added to a solution of $[N(PPh_3)_2][Ru_4H(CO)_{12}BH]$ (58 mg, 0.045 mmol) in CH_2Cl_2 (5 cm^3). After 5 h of stirring at room temperature the solution turned from orange to dark brown. Products were separated by TLC (hexane–CH_2Cl_2 1:1) and two major fractions (red-brown, $R_f \approx 0.8$; orange-yellow, broad, extending from the baseline) were collected; several very weak bands were also visible on the TLC plate. The second fraction was a mixture the components of which could not be characterised. The red-brown fraction was identified as $[RhRu_4H_2(\eta^5\text{-}C_5Me_5)(\mu\text{-}Cl)(CO)_{12}B]$ **1** (yield ≈ 20%). NMR (CD_2Cl_2, 298 K): ^1H (400 MHz), δ +1.78 (s, C_5Me_5), −5.6 (br, Ru–H–B) and −18.60 (s, Ru–H–Ru); ^{11}B (128 MHz), δ +155.

* Basis of the presentation given at Dalton Discussion No. 1, 3rd–5th January 1996, University of Southampton, UK.

Non-SI unit employed: atm = 101 325 Pa.

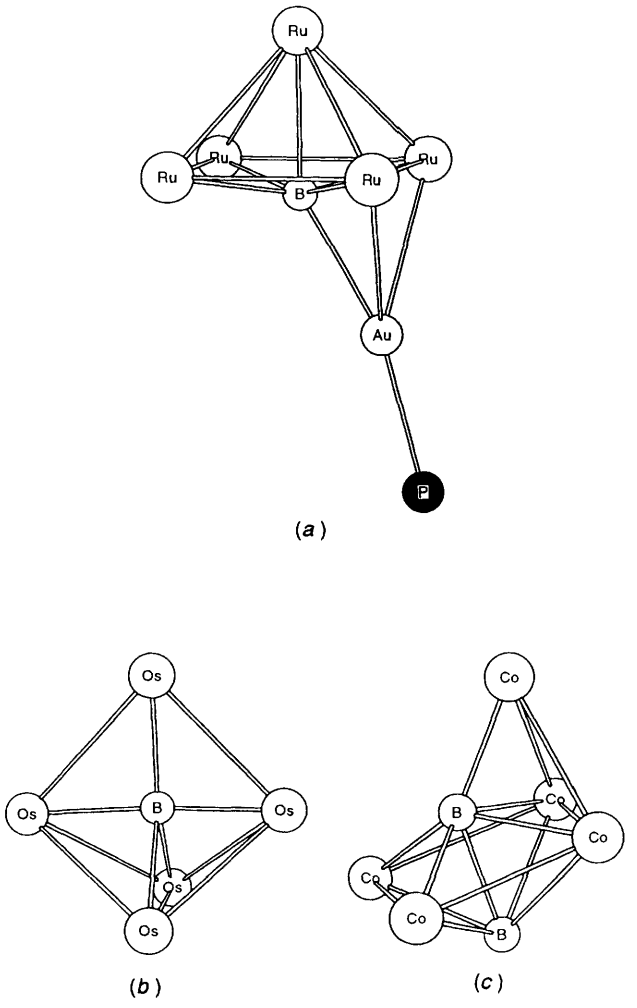

Fig. 1 The core structures of (*a*) $[Ru_5(CO)_{15}B(AuPPh_3)]$,[4] (*b*) $[Os_5H(CO)_{16}B]$ [5] and (*c*) $[Co_5(CO)_{14}B(BH)]$.[6] The structures have been drawn using the published atomic coordinates, obtained through the Cambridge Crystallographic Data Base, implemented through the ETH, Zürich [7]

IR (CH_2Cl_2, cm^{-1}): ν_{CO} 2085m, 2061vs, 2040s, 2030s, 2001m, and 1985m. FAB mass spectrum *m/z* 1026 (M^+) with 12 CO losses (calc. for $^{12}C_{22}{}^1H_{17}{}^{11}B^{35}Cl^{16}O_{12}{}^{103}Rh^{101}Ru_4$: 1026).

Reaction of $[\{Ir(\eta^5\text{-}C_5Me_5)Cl_2\}_2]$ with $[N(PPh_3)_2][Ru_4H(CO)_{12}BH]$

The dimer $[\{Ir(\eta^5\text{-}C_5Me_5)Cl_2\}_2]$ (36 mg, 0.045 mmol) was added to a solution of $[N(PPh_3)_2][Ru_4H(CO)_{12}BH]$ (64 mg, 0.05 mmol) in CH_2Cl_2 (5 cm^3). After 5 h of stirring at room temperature the solution turned dark brown, but attempts to separate products by TLC yielded only intractable material.

Reaction of $[N(PPh_3)_2][Ru_4H(CO)_{12}BH]$ with $[\{Rh(nbd)Cl\}_2]$ and $[Au(PPh_3)Cl]$

The dimer $[\{Rh(nbd)Cl\}_2]$ (28 mg, 0.06 mmol) was added to a solution of $[N(PPh_3)_2][Ru_4H(CO)_{12}BH]$ (103 mg, 0.08 mmol) in CH_2Cl_2 (5 cm^3). After 3 min at room temperature an excess of $[Au(PPh_3)Cl]$ was added to the stirred solution and the solvent volume was immediately reduced *in vacuo*. Products were separated by TLC (hexane–CH_2Cl_2, 2:1) and five major fractions were eluted leaving an orange-brown intractable baseline. The products were identified as $[Ru_4H_3(CO)_{12}(AuPPh_3)]$ [10] ($R_f \approx 0.8$, 10%), *cis*-$[Rh_2Ru_4H(nbd)_2(CO)_{12}B]$ [11] (brown, $R_f \approx 0.7$, ≈5%), $[RhRu_4H(nbd)(CO)_{12}B(AuPPh_3)]$ **2** (brown, $R_f \approx 0.65$, ≈20%), *cis*-$[Rh_2Ru_4(nbd)(CO)_{14}B(AuPPh_3)]$ (tan, $R_f \approx 0.55$, ≈5%) [11] and *cis*-$[Rh_2Ru_4(nbd)_2(CO)_{12}B(AuPPh_3)]$ (red-brown, $R_f \approx 0.45$, ≈10%).[11] The product distribution is influenced by the reaction time; if the $[Au(PPh_3)Cl]$ is not added quickly the yields of *cis*-$[Rh_2Ru_4(nbd)(CO)_{14}B(AuPPh_3)]$ and *cis*-$[Rh_2Ru_4(nbd)_2(CO)_{12}B(AuPPh_3)]$ increase (to around 25% if the time lapse is 30 min) at the expense of compound **2**. NMR for **2** (298 K): ^1H (400 MHz, $CDCl_3$), δ +7.7–7.4 (m, 15 H, Ph), +4.46 (4 H, nbd, see text), +3.21 (br, nbd, see text), +1.30 (2 H, nbd) and −18.93 (s, Ru–H–Ru); ^{11}B (128 MHz, CD_2Cl_2), δ +171 (d, J_{RhB} 25 Hz); ^{31}P (162 MHz, $CDCl_3$), δ +54.8 (br). IR (CH_2Cl_2, cm^{-1}): ν_{CO} 2071m, 2029vs, 2006s, 1993m (sh), 1960m and 1872w. FAB mass spectrum: *m/z* 1317 ($M^+ - 3CO$)(calc.for $^{12}C_{37}{}^1H_{24}{}^{197}Au^{11}B^{16}O_{12}{}^{31}P^{103}Rh^{101}Ru_4$: 1406).

Preparations of $[RhRu_4H(nbd)(CO)_{12}B\{AuP(C_6H_{11})_3\}]$ and $[RhRu_4H(nbd)(CO)_{12}B\{AuP(C_6H_4Me\text{-}2)_3\}]$

These compounds were prepared in analogous manners to compound **2** with the respective phosphine gold(I) chloride substituted in place of $[Au(PPh_3)Cl]$. The product distribution was similar in each case, and is similarly influenced by the reaction time.

$[RhRu_4H(nbd)(CO)_{12}B\{AuP(C_6H_{11})_3\}]$ **3**: NMR (298 K, CD_2Cl_2) ^1H (400 MHz), δ +4.54 (4 H, nbd), +3.83 (br, nbd, see text), +2.3–1.1 (m, 33 H, C_6H_{11}) and −18.86 (s, Ru–H–Ru); ^{11}B (128 MHz), δ +171 (br); ^{31}P (162 MHz), δ +72.6 (br); IR (CH_2Cl_2, cm^{-1}) ν_{CO} 2062w, 2021vs, 1982m (sh) and 1867w; FAB mass spectrum: *m/z* 1426 (M^+) (calc. for $^{12}C_{37}{}^1H_{42}{}^{197}Au^{11}B^{16}O_{12}{}^{31}P^{103}Rh^{101}Ru_4$: 1424).

$[RhRu_4H(nbd)(CO)_{12}B\{AuP(C_6H_4Me\text{-}2)_3\}]$ **4**: NMR (298 K, $CDCl_3$): ^1H (400 MHz), δ +7.74–7.25 (m, 12 H, aryl), +4.31 (nbd, 4 H, see text), +3.0 (br, nbd, see text), +2.41 (s, 9 H, Me), +1.3 (s, 2 H, nbd) and −18.84 (s, Ru–H–Ru); ^{11}B (128 MHz), δ +166 (br); ^{31}P (162 MHz), δ +51.7 (br); IR (CH_2Cl_2, cm^{-1}) ν_{CO} 2070m, 2028vs, 2006m and 1965m; FAB mass spectrum *m/z* 1426 (M^+) (calc. for $^{12}C_{37}{}^1H_{42}{}^{197}Au^{11}B^{16}O_{12}{}^{31}P^{103}Rh^{101}Ru_4$: 1424).

Reactions of compounds 2 and 3 with CO

A solution of compound **2** (8 mg, 6 μmol) in CH_2Cl_2 (25 cm^3) was stirred under a pressure of 60 atm CO (room temperature) for 20 h. After reducing the volume to 2 cm^3, the products were separated by TLC (hexane-CH_2Cl_2, 9:7). Several weak fractions were observed in addition to one major brown band (R_f 0.7, ≈40%) characterised as $[RhRu_4H(CO)_{14}B(AuPPh_3)]$. NMR (298 K, CD_2Cl_2): ^1H(400 MHz), δ +7.7–7.4 (m, 15 H, Ph) and −18.80 (s, Ru–H–Ru); ^{11}B (128 MHz), δ +166 (br). IR (CH_2Cl_2, cm^{-1}): ν_{CO} 2089w, 2059s, 2045vs, 2023m and 1984mw. FAB mass spectrum: *m/z* 1371 (M^+) (calc. for $^{12}C_{32}{}^1H_{16}{}^{197}Au^{11}B^{16}O_{14}{}^{31}P^{103}Rh^{101}Ru_4$: 1370).

In a similar reaction a solution of compound **3** (37 mg, 26 μmol) in CH_2Cl_2 (30 cm^3) reacted with CO (50 atm) at room temperature for 13 h. Separation by TLC (hexane–CH_2Cl_2, 3:2) gave two main products: brown $[RhRu_4H(CO)_{14}B\{AuP(C_6H_{11})_3\}]$ (R_f 0.7, ≈70%) and an orange compound (R_f 0.6) that could not be fully characterised.

$[RhRu_4H(CO)_{14}B\{AuP(C_6H_{11})_3\}]$: NMR (298 K): ^1H (400 MHz, CD_2Cl_2), δ +2.3–1.3 (m, C_6H_{11}) and −18.80 (s, Ru–H–Ru); ^{11}B (128 MHz, $CDCl_3$), δ +171 (br); IR (CH_2Cl_2, cm^{-1}) ν_{CO} 2088w, 2055s, 2043vs, 2021s, 1980mw and 1895vw; FAB mass spectrum: *m/z* 1390 (M^+) (calc. for $^{12}C_{32}{}^1H_{34}{}^{197}Au^{11}B^{16}O_{14}{}^{31}P^{103}Rh^{101}Ru_4$: 1388).

Crystal structure determinations

Crystallographic data for $[RhRu_4H_2(\eta^5\text{-}C_5Me_5)(\mu\text{-}Cl)(CO)_{12}B]$ **1** and $[RhRu_4H(nbd)(CO)_{12}B(AuPPh_3)]$ **2** are collected in Table 1. Crystals were photographically characterised and determined to belong to the triclinic system for **1** and

Table 1 Crystallographic data[a] for $[RhRu_4H_2(\eta^5\text{-}C_5Me_5)(\mu\text{-}Cl)(CO)_{12}B]$ **1** and $[RhRu_4H(nbd)(CO)_{12}B(AuPPh_3)]$ **2**

Formula	$C_{22}H_{17}BClO_{12}RhRu_4$	$C_{37}H_{24}AuBO_{12}PRhRu_4$
Formula weight	1026.8	1406.5
Crystal system	Triclinic	Monoclinic
Space group	$P\bar{1}$	$P2_1/n$
a/Å	8.533(2)	15.274(3)
b/Å	10.763(3)	17.634(4)
c/Å	16.745(4)	16.156(3)
α/°	98.24(2)	—
β/°	95.45(2)	110.30(2)
γ/°	102.71(2)	—
U/Å^3	1471.8(5)	4081.3(15)
Z	2	4
Crystal dimensions/mm	0.10 × 0.35 × 0.40	0.12 × 0.32 × 0.36
Crystal colour	Red-brown	Dark red
D_c/g cm^3	2.317	2.289
μ(Mo-Kα)/cm^{-1}	27.0	55.2
F(000)	976	2648
T/K	233	296
T_{max}/T_{min}	1.80	1.82
2θ scan range/°	4–60	4–48
Data collected (h, k, l)	±12, ±15, +23	±17, +20, +18
Reflections collected	8833	6656
Independent reflections	8567	6407
Observed reflections $[F_o \geqslant n\sigma(F_o)]$	6618 (n = 5)	4183 (n = 4)
R^b	0.0331 (0.0464)[c]	0.0468 (0.0829)[c]
R'^b	0.0476 (0.0527)[c]	0.0519 (0.0615)[c]
g In weighting scheme w	0.0008	0.0010
Δ/σ (max.)	0.04	0.003
$\Delta(\rho)$/e Å^{-3}	1.16	1.07
N_o/N_v	17.5	8.1
Goodness of fit	1.15	0.99

[a] Details in common: Siemens P4 diffractometer; graphite monochromated Mo-Kα radiation (λ = 0.071 073 Å); three standard reflections every 197. [b] Quantity minimised = $\Sigma w\Delta^2$; $R = \Sigma\Delta/\Sigma(F_o)$; $R' = \Sigma\Delta w^{\frac{1}{2}}/\Sigma(F_o w^{\frac{1}{2}})$, $\Delta = |F_o - F_c|$; $w^{-1} = \sigma^2(F) + gF^2$. [c] All data.

the monoclinic crystal system for **2**. The centrosymmetric alternative was selected for **1** based on the results of refinement, and systematic absences in the diffraction data for **2** uniquely determined its space group. Azimuthal scans indicated that corrections for absorption were required and semi-empirical methods were applied. The structures were solved by direct methods, completed from Fourier-difference maps, and refined with anisotropic thermal parameters for all non-hydrogen atoms. Hydridic hydrogen atoms were crystallographically found and refined; the remaining hydrogen atoms were placed in idealised locations. All computations used SHELXTL 4.2 software.[12]

Complete atomic coordinates, thermal parameters and bond lengths and angles have been deposited at the Cambridge Crystallographic Data Centre. See Instructions for Authors, *J. Chem. Soc., Dalton Trans.*, 1996, Issue 1.

Results and Discussion

Synthesis and spectroscopic characterisation of $[RhRu_4H_2(\eta^5\text{-}C_5Me_5)(\mu\text{-}Cl)(CO)_{12}B]$ 1

Recently we reported the formation of the unusual spiked-butterfly cluster $[RhRu_4H(\eta^5\text{-}C_5Me_5)(CO)_{13}BH_2]$ as a minor product in the reactions of $[Ru_3(CO)_9BH_4]^-$ and $[Ru_3(CO)_9B_2H_5]^-$ with $[\{Rh(\eta^5\text{-}C_5Me_5)Cl_2\}_2]$.[13] The reaction pathway must involve not only the addition of the rhodium fragment to the cluster, but also the expansion of the Ru_3B core to a Ru_4B butterfly framework. *In situ* $Ru_3B \longrightarrow Ru_4B$ assemblies of this type are not unprecedented and one interesting example is the formation of $[Ru_4H(CO)_{12}BH(\mu\text{-}NCHMe)]$ during the photolysis of $[Ru_3(CO)_9BH_5]$ in MeCN in the presence of $[M(CO)_6]$ (M = Cr, Mo or W); notably however, MeCN does *not* appear to add directly to $[Ru_4H(CO)_{12}BH_2]$ to give $[Ru_4H(CO)_{12}BH(\mu\text{-}NCHMe)]$.[14] In the first part of this paper we report the results of the direct reaction between $[Ru_4H(CO)_{12}BH]^-$ and $[\{Rh(\eta^5\text{-}C_5Me_5)Cl_2\}_2]$.

The dimer $[\{Rh(\eta^5\text{-}C_5Me_5)Cl_2\}_2]$ may formally be a source either of a $\{Rh(\eta^5\text{-}C_5Me_5)\}^{2+}$ or a $\{Rh(\eta^5\text{-}C_5Me_5)Cl\}^+$ fragment. The reaction of $[RuH_4(CO)_{12}BH]^-$ with 1 equivalent of $[\{Rh(\eta^5\text{-}C_5Me_5)Cl_2\}_2]$ yielded compound **1** as the only characterisable product. In the ^{11}B NMR spectrum a signal at δ +155 suggests that the environment about the boron atom may be intermediate between that of a neutral M_4B butterfly (semi-interstitial, typically $\delta \approx 110$) and a M_6B cage (interstitial, typically $\delta \approx 195$–200).[1,2] In the ^1H NMR spectrum a singlet at δ +1.78 is consistent with the presence of the C_5Me_5 ligand, whilst a sharp singlet and a broad resonance at δ −18.60 and −5.6, respectively, are indicative of Ru–H–Ru and Ru–H–B protons respectively. However, no ^{11}B–^1H coupling could be resolved in the ^{11}B NMR spectrum. The isotopic distribution of the parent envelope (m/z 1026) in the FAB mass spectrum of **1** is consistent with a formulation of $[RhRu_4H_2(C_5Me_5)Cl(CO)_{12}B]$ and this has been confirmed by the results of an X-ray diffraction study. Attempts to synthesise an iridium analogue of compound **1** were unsuccessful; no characterisable product of the reaction between $[RuH_4(CO)_{12}BH]^-$ and $[\{Ir(\eta^5\text{-}C_5Me_5)Cl_2\}_2]$ was obtained.

Crystal structure and formation of $[RhRu_4H_2(\eta^5\text{-}C_5Me_5)(\mu\text{-}Cl)(CO)_{12}B]$ 1

Crystals of compound **1**, suitable for X-ray analysis, were grown from a CH_2Cl_2 solution layered with hexane. The molecular structure is shown in Fig. 2 and the structure of the cluster core in Fig. 3. Selected bond distances and angles are listed in Table 2. The five metal atoms define an unusual 'envelope' (or edge-bridged square) skeleton which is consistent with a 78 valence-electron (v.e.) count [64(square) + 48(triangle) − 34(shared edge)]. The framework is supported internally

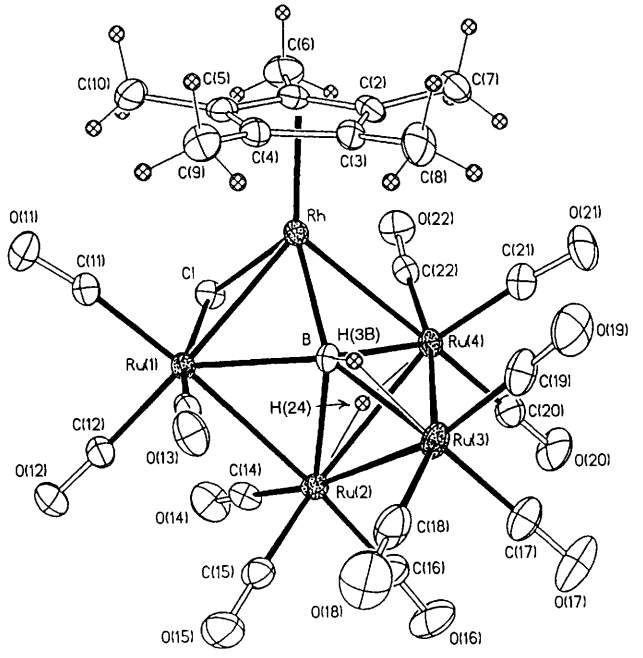

Fig. 2 Molecular structure of $[RhRu_4H_2(\eta^5\text{-}C_5Me_5)(\mu\text{-}Cl)(CO)_{12}B]$ **1**

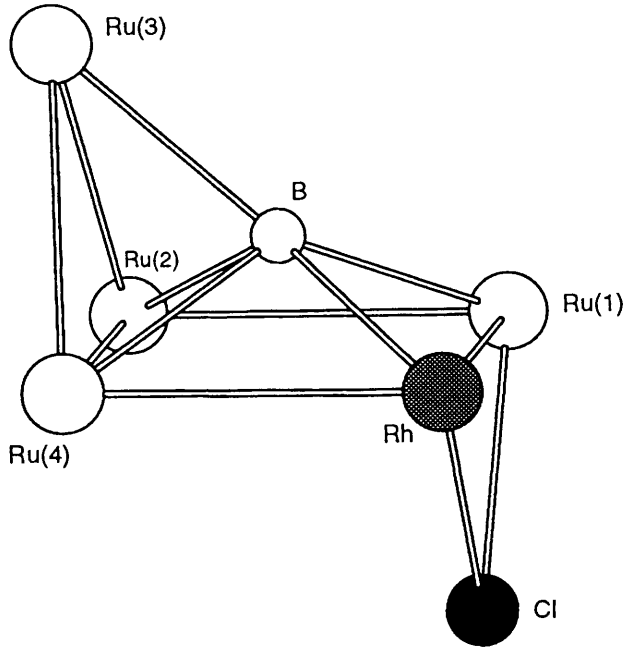

Fig. 3 Core of compound **1** showing the 'envelope' pentametal skeleton

by the interstitial boron atom, and externally by a bridging chloride ligand along the edge Rh–Ru(1) [Rh–Cl 2.408(1), Ru(1)–Cl 2.442(1) Å]. The Rh–B distance is 2.122(5) Å and the Ru–B distances lie in the range 2.198(4)–2.275(5) Å indicating that there is bonding contact between the boron atom and all five metal atoms. The cluster core geometry is not unlike that observed for $[Co_5(CO)_{14}B(BH)]$ [Fig. 1(*c*)] although here there is an additional BH unit interacting with both the interstitial boron atom and the rhomboidal Co_4 face.[6]

The metal–metal edge bridged by the chloride ligand is the shortest edge in the $RhRu_3$ rhombus [Rh–Ru(1) 2.723(1) compared to Rh–Ru(4) 2.844(1), Ru(1)–Ru(2) 2.876(1) and Ru(2)–Ru(4) 2.920(1) Å] and is also shorter than the remaining two Ru–Ru edges [Ru(2)–Ru(3) 2.826(1), Ru(3)–Ru(4) 2.812(1) Å]. Similar shortening of Ru–Ru bonds in clusters in which both Cl-bridged and -unbridged bond lengths can be compared has been observed previously[15] and the phenomenon

Table 2 Selected bond distances (Å) and angles (°) for compound **1**

Rh–Ru(1)	2.723(1)	Rh–Ru(4)	2.844(1)
Rh–Cl	2.408(1)	Rh–B	2.122(5)
Ru(1)–Ru(2)	2.876(1)	Ru(1)–Cl	2.442(1)
Ru(1)–B	2.250(5)	Ru(2)–Ru(3)	2.826(1)
Ru(2)–Ru(4)	2.920(1)	Ru(2)–B	2.275(5)
Ru(3)–Ru(4)	2.812(1)	Ru(3)–B	2.219(5)
Ru(4)–B	2.198(4)	Ru(2)–H(24)	1.99(5)
Ru(4)–H(24)	1.71(5)	Ru(3)–H(3B)	1.68(5)
B–H(3B)	1.17(5)		
Ru(1)–Rh–Ru(4)	93.6(1)	Ru(1)–Rh–Cl	56.4(1)
Ru(4)–Rh–Cl	91.8(1)	Ru(1)–Rh–B	53.6(1)
Ru(4)–Rh–B	50.0(1)	Cl–Rh–B	91.5(1)
Rh–Ru(1)–Ru(2)	90.3(1)	Rh–Ru(1)–Cl	55.3(1)
Ru(2)–Ru(1)–Cl	89.0(1)	Rh–Ru(1)–B	49.4(1)
Ru(2)–Ru(1)–B	50.9(1)	Cl–Ru(1)–B	87.7(1)
Ru(1)–Ru(2)–Ru(3)	93.7(1)	Ru(1)–Ru(2)–Ru(4)	88.9(1)
Ru(3)–Ru(2)–Ru(4)	58.6(1)	Ru(1)–Ru(2)–B	50.2(1)
Ru(3)–Ru(2)–B	50.2(1)	Ru(4)–Ru(2)–B	48.1(1)
Ru(2)–Ru(3)–Ru(4)	62.4(1)	Ru(2)–Ru(3)–B	51.9(1)
Ru(4)–Ru(3)–B	50.1(1)	Rh–Ru(4)–Ru(2)	87.1(1)
Rh–Ru(4)–Ru(3)	93.8(1)	Ru(2)–Ru(4)–Ru(3)	59.0(1)
Rh–Ru(4)–B	47.7(1)	Ru(2)–Ru(4)–B	50.4(1)
Ru(3)–Ru(4)–B	50.8(1)	Rh–Cl–Ru(1)	68.3(1)
Rh–B–Ru(1)	77.0(2)	Rh–B–Ru(2)	129.2(2)
Rh–B–Ru(3)	144.1(3)	Rh–B–Ru(4)	82.3(2)
Ru(1)–B–Ru(2)	78.9(2)	Ru(1)–B–Ru(3)	137.2(2)
Ru(2)–B–Ru(3)	77.9(2)	Ru(1)–B–Ru(4)	131.8(2)
Ru(2)–B–Ru(4)	81.5(2)	Ru(3)–B–Ru(4)	79.1(2)

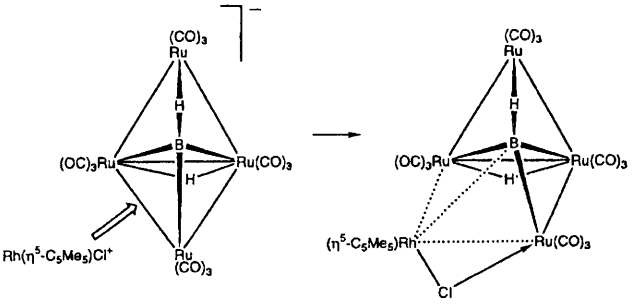

Scheme 1 Schematic representation of the formation of compound **1** by the insertion of a $\{Rh(\eta^5\text{-}C_5Me_5)Cl\}^+$ fragment into one Ru_{hinge}–$Ru_{wingtip}$ edge of the butterfly precursor

has been examined in Ru_3 systems using the Fenske–Hall molecular orbital (MO) approach;[16] interactions between the Ru_3 framework and the tangential 3p atomic orbital (AO) of the chloride ligand appear to be critically important. However, in some systems such as $[Ru_3(CO)_{10}(\mu\text{-}Cl)(\mu\text{-}AuPPh_3)]$ in which both the chloride and gold(I) moiety bridge the same edge, the result is one of lengthening and this has been attributed to the predominant effect of the $AuPPh_3$ unit.[17]

The two cluster hydrogen atoms in compound **1** have been located and bridge edges Ru(3)–B and Ru(2)–Ru(4). These environments are consistent with the observed ^1H NMR spectroscopic data of δ −5.6 (br, Ru–H–B) and −18.60 (s, Ru–H–Ru).

Formally we can view compound **1** as originating from the insertion of an $(\eta^5\text{-}C_5Me_5)RhCl$ unit into one Ru_{hinge}–$Ru_{wingtip}$ edge of the butterfly core of $[Ru_4H(CO)_{12}BH]^-$ and this is represented in Scheme 1. Formation of a Rh–B interaction is concomitant with the formation of two Ru–Rh interactions and the additional electrons provided by the chloride ligand (depicted in Scheme 1 as a formal Cl→Ru co-ordinate bond) complete the 78 v.e. count required by the 'envelope' pentametal framework. The internal dihedral angle between the planes containing the Ru(2), Ru(3), Ru(4) and Rh, Ru(1), Ru(2), Ru(4) atoms is 95.6° and that between the planes containing the atoms Rh, Ru(1), Ru(2), Ru(4) and Rh, Ru(1),

Cl is 90.8°. The former angle may be compared with the internal dihedral angle of the butterfly precursor (see discussion below and Scheme 1) with the edge Ru(2)–Ru(4) originating from the hinge of the Ru_4B butterfly. The crystal structure of the anion $[RuH_4(CO)_{12}BH]^-$ has not been determined but in $[RuH_4(CO)_{12}BH]$[18] the internal dihedral angle is 118°. It is reasonable to say that the interstitial boron atom plays an important structural role in supporting the metal skeleton during the cluster expansion. In compound **1** the longest metal–metal bond is Ru(2)–Ru(4) [2.920(1) Å] and this is similar to the hinge Ru–Ru bond distance in $[RuH_4(CO)_{12}BH]$ [2.904(1) Å].[18]

Reaction of $[RuH_4(CO)_{12}BH]^-$ with $[\{Rh(nbd)Cl\}_2]$ in the presence of a gold(I) phosphine

The expansion of the metal framework around the semi-interstitial boron atom in $[RuH_4(CO)_{12}BH]^-$ has led to the formation of the octahedral carbonyl clusters $[Rh_2Ru_4(CO)_{16}B]^-$ and $[Ir_2Ru_4(CO)_{16}B]^-$ which react further with gold(I) phosphines to give *cis*- and *trans*-$[Rh_2Ru_4(CO)_{16}B(AuPR_3)]$ and *cis*-$[Ir_2Ru_4(CO)_{16}B(AuPR_3)]$ (R = Ph or C_6H_{11}).[19] Although Fehlner and co-workers[20] have evidenced the formation of a pentametal intermediate cluster during the reactions of $[Fe_4H(CO)_{12}BH]^-$ with $[\{Rh(CO)_2Cl\}_2]$ which ultimately gives *cis*- and *trans*-$[Fe_4Rh_2(CO)_{16}B]^-$, we did not observe such an intermediate in the reactions of $[RuH_4(CO)_{12}BH]^-$ with $[\{M(CO)_2Cl\}_2]$ (M = Rh or Ir).[19] The reaction of $[RuH_4(CO)_{12}BH]^-$ with $[\{Rh(nbd)Cl\}_2]$ produces octahedral clusters $[Rh_2Ru_4(nbd)_2(CO)_{12}B]^-$, $[Rh_2Ru_4H(nbd)_2(CO)_{12}B]$ and $[Rh_2Ru_4(nbd)(CO)_{14}B]^-$ depending upon the conditions.[11] Provided that the Group 9 metal fragments add sequentially to $[RuH_4(CO)_{12}BH]^-$, products with a $RhRu_4B$ core should be accessible through a carefully controlled reaction between $[RuH_4(CO)_{12}BH]^-$ and $[\{Rh(nbd)Cl\}_2]$. The following discussion illustrates how gold(I) phosphine fragments may be used to trap a $RhRu_4B$-containing cluster before further expansion to the octahedral Ru_2Ru_4B occurs.

When [Au(PPh$_3$)Cl] is added to a CH_2Cl_2 solution containing the anion $[Ru_4H(CO)_{12}BH]^-$ and $[\{Rh(nbd)Cl\}_2]$ which have been allowed to react together for about 30 min, the principal products are *cis*-$[Rh_2Ru_4(nbd)(CO)_{14}B(AuPPh_3)]$ and *cis*-$[Rh_2Ru_4(nbd)_2(CO)_{12}B(AuPPh_3)]$.[11] A similar result is obtained with either $[Au\{P(C_6H_{11})_3\}Cl]$ or $[Au\{P(C_6H_4Me\text{-}2)_3\}Cl]$. However, if the gold(I) phosphine is added no more than 3 min after the addition of $[\{Rh(nbd)Cl\}_2]$ to the anion $[Ru_4H(CO)_{12}BH]^-$ the product distribution is altered significantly and yields of about 20% of $[RhRu_4H(nbd)(CO)_{12}B(AuPR_3)]$ (R = Ph, C_6H_{11} or 2-MeC_6H_4) can be isolated.

The solution ^{11}B NMR spectrum of $[RhRu_4H(nbd)(CO)_{12}B(AuPPh_3)]$ **2** (298 K) shows a signal at δ +171 which is a doublet (*J* 25 Hz); this coupling pattern persists in the $^{11}B\{^1H\}$ spectrum and is assigned to ^{103}Rh–^{11}B spin coupling. The magnitude of the coupling is similar to that observed in $[Ru_4Rh_2(CO)_{16}B]^-$ (triplet, J_{RhB} 26 Hz).[19] The resonance for **2** is close to that observed (δ +172.5) for $[Ru_5(CO)_{15}B(AuPPh_3)]$[4] and therefore suggests a similar (but not necessarily identical) environment for the boron atom. The ^{1}H NMR spectrum of compound **2** indicates the presence of both phenyl (the PPh_3 ligand, supported by the ^{31}P NMR spectrum) and norbornadiene protons, and the relative integrals of the signals confirmed a ratio of PPh_3: nbd ligands of 1 : 1. This is in accord with the mass spectrum. The structural details of cluster **2** were confirmed by the results of an X-ray diffraction study (see below).

The solution NMR spectroscopic signatures of the products of the reactions of $[Au(PR_3)Cl]$ (R = C_6H_{11} or 2-MeC_6H_4) with $[Ru_4H(CO)_{12}BH]^-$ and $[\{Rh(nbd)Cl\}_2]$ were similar to those of compound **2** allowing the products to be formulated as $[RhRu_4H(nbd)(CO)_{12}B\{AuP(C_6H_{11})_3\}]$ **3** and $[RhRu_4H(nbd)(CO)_{12}B\{AuP(C_6H_4Me\text{-}2)_3\}]$ **4**. The variable-temperature ^{1}H NMR spectra of compounds **2**–**4** are discussed below.

Crystal structure and formation of $[RhRu_4H(nbd)(CO)_{12}B(AuPPh_3)]$ 2

Crystals of compound **2**, suitable for X-ray analysis, were grown by slow diffusion of EtOH into a CH_2Cl_2 solution of the compound. The molecular structure is shown in Fig. 4, and the structure of the cluster core in Fig. 5. Selected bond distances and angles are listed in Table 3. The structural determination confirms that the reaction strategy was successful in trapping a cluster with a $RhRu_4B$ core. The presence of the nbd ligand effectively 'labels' the rhodium site and allows the rhodium and ruthenium atoms to be readily distinguished in the structural analysis; the presence of the single rhodium atom is consistent with the ^{11}B NMR spectroscopic data described above. The cluster geometry of compound **2** bears a striking similarity to that of $[Ru_5(CO)_{15}B(AuPPh_3)]$[4] shown in Fig. 1(*a*). In **2**, the ruthenium and rhodium atoms define a square-based pyramid with the Rh atom occupying one of the basal sites; the Ru_4 butterfly residue of the starting anion is thus retained. The boron atom is within bonding contact of all five of these metal atoms although the distance to the apex [Ru(2)–B 2.29(2) Å] is greater than to the basal metal atoms [M_{basal}–B range 2.05–2.16(2) Å]; the boron atom is 0.32 Å below the square plane containing the Rh, Ru(1), Ru(3) and Ru(4) atoms, and this compares with a corresponding displacement of 0.375 Å in $[Ru_5(CO)_{15}B(AuPPh_3)]$.[4] The $AuPPh_3$ unit bridges the edge Ru(1)–Rh but also interacts with the boron centre [Au–B 2.26(2) Å].

One cluster hydrogen atom was located crystallographically. It bridges the edge Ru(2)–Ru(4) and this site is consistent with the appearance in the ^{1}H NMR spectrum of a singlet at δ − 18.93.

The observation that the butterfly Ru_4B motif of the starting material is present in compound **2** allows us to propose a route by which the reaction may proceed and this is summarised in Scheme 2. We envisage initial addition of one {Rh(nbd)} fragment to give an intermediate compound of the type '$[RhRu_4H(nbd)(CO)_{12}B]^-$' or the conjugate acid thereof. This could react with [Au(PPh$_3$)Cl] to generate compound **2**, or undergo further reaction with $[\{Rh(nbd)Cl\}_2]$ to give the observed octahedral clusters with a *cis* arrangement of rhodium centres.[11] We have shown that altering the reaction conditions can tip the balance in favour of one of these competitive pathways, but the presence of the phosphinegold(I) chloride in the *early stages* of the reaction is clearly essential for the formation of compound **2**.

Solution dynamics of $[RhRu_4H(nbd)(CO)_{12}B(AuPR_3)]$ (R = Ph, C_6H_{11} or 2-MeC_6H_4)

In the solid state all eight hydrogen atoms of the nbd ligand are inequivalent (Fig. 4). In the ^{1}H NMR spectrum (at 298 K, in CD_2Cl_2) compound **2** shows two signals at δ +4.46 and +3.21 assigned to the olefinic and bridgehead protons respectively and one at δ +1.30 assigned to the two methylene protons; these data indicate that the system is fluxional. Cooling the sample [Fig. 6(*c*)] results in collapse of the signals at δ +4.46 and +3.21, and at 206 K four sharp signals are resolved at δ 4.73 (2 H), 4.13 (2 H), 3.72 (1 H) and 2.41 (1 H) whilst that at δ +1.30 remains unaffected. These results may be explained in terms of the existence of two dynamic processes: (*a*) a facile rocking motion of the $AuPPh_3$ unit and (*b*) rotation of the nbd ligand. Fig. 6(*a*) shows that with the rocking of the $AuPPh_3$ unit as the only process the two methylene protons c and c′ are equivalent on the NMR spectroscopic time-scale, the bridgehead protons are inequivalent (d and e) and the four olefinic protons appear as two sets of two (a and a′, and b and b′). [Of course, instead of

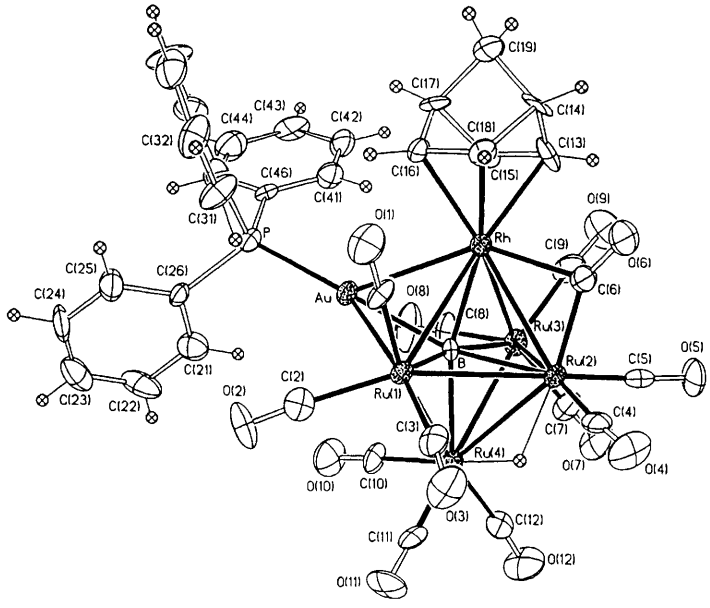

Fig. 4 Molecular structure of $[RhRu_4H(nbd)(CO)_{12}B(AuPPh_3)]$ **2**

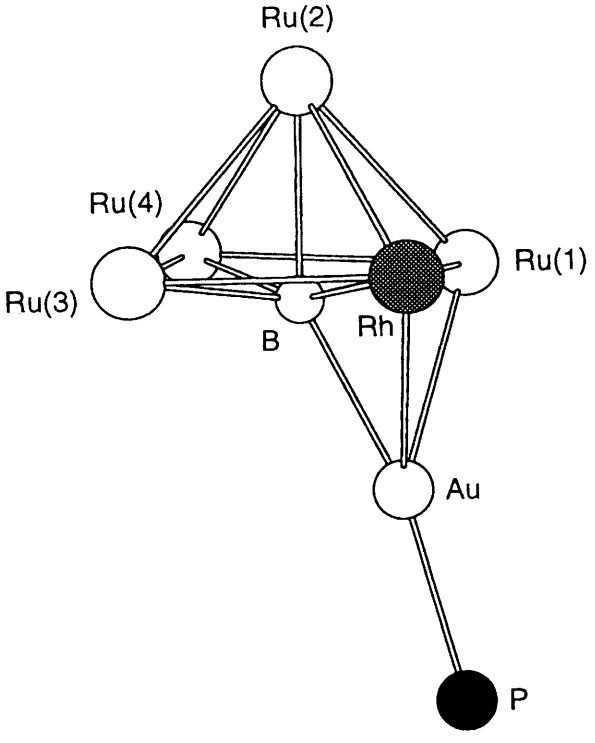

Fig. 5 Core of compound **2** drawn in the same orientation as that of $[Ru_5H(CO)_{15}B(AuPPh_3)]$[4] shown in Fig. 1(*a*)

Table 3 Selected bond distances (Å) and angles (°) for $[RhRu_4H(nbd)(CO)_{12}B(AuPPh_3)]$ **2**

Au–Rh	2.817(1)	Au–Ru(1)	2.756(1)
Au–P	2.302(4)	Au–B	2.26(2)
Rh–Ru(1)	3.030(2)	Rh–Ru(2)	2.836(2)
Rh–Ru(3)	2.951(2)	Rh–B	2.13(2)
Ru(1)–Ru(2)	2.896(2)	Ru(1)–Ru(4)	2.897(2)
Ru(1)–B	2.09(2)	Ru(2)–Ru(3)	2.856(2)
Ru(2)–Ru(4)	2.888(2)	Ru(2)–B	2.29(2)
Ru(3)–Ru(4)	2.906(2)	Ru(3)–B	2.05(2)
Ru(4)–B	2.16(2)	Ru(2)–H(24)	1.84(4)
Ru(4)–H(24)	1.47(4)		
Rh–Au–Ru(1)	65.9(1)	Rh–Au–P	134.8(1)
Ru(1)–Au–P	142.9(1)	Rh–Au–B	48.0(4)
Ru(1)–Au–B	47.9(4)	P–Au–B	168.0(4)
Au–Rh–Ru(1)	56.1(1)	Au–Rh–Ru(2)	102.6(1)
Ru(1)–Rh–Ru(2)	59.1(1)	Au–Rh–Ru(3)	79.2(1)
Ru(1)–Rh–Ru(3)	86.5(1)	Ru(2)–Rh–Ru(3)	59.1(1)
Au–Rh–B	52.2(5)	Ru(1)–Rh–B	43.5(4)
Ru(2)–Rh–B	52.5(5)	Ru(3)–Rh–B	44.0(4)
Au–Ru(1)–Rh	58.0(1)	Au–Ru(1)–Ru(2)	102.5(1)
Rh–Ru(1)–Ru(2)	57.1(1)	Au–Ru(1)–Ru(4)	84.4(1)
Rh–Ru(1)–Ru(4)	91.0(1)	Ru(2)–Ru(1)–Ru(4)	59.8(1)
Au–Ru(1)–B	53.5(5)	Rh–Ru(1)–B	44.5(4)
Ru(2)–Ru(1)–B	51.5(5)	Ru(4)–Ru(1)–B	48.2(5)
Rh–Ru(2)–Ru(1)	63.8(1)	Rh–Ru(2)–Ru(3)	62.5(1)
Ru(1)–Ru(2)–Ru(3)	90.9(1)	Rh–Ru(2)–Ru(4)	95.3(1)
Ru(1)–Ru(2)–Ru(4)	60.1(1)	Ru(3)–Ru(2)–Ru(4)	60.8(1)
Rh–Ru(2)–B	47.6(4)	Ru(1)–Ru(2)–B	45.6(4)
Ru(3)–Ru(2)–B	45.4(4)	Ru(4)–Ru(2)–B	47.7(4)
Rh–Ru(3)–Ru(2)	58.4(1)	Rh–Ru(3)–Ru(4)	92.5(1)
Ru(2)–Ru(3)–Ru(4)	60.1(1)	Rh–Ru(3)–B	46.1(4)
Ru(2)–Ru(3)–B	52.5(4)	Ru(4)–Ru(3)–B	48.0(5)
Ru(1)–Ru(4)–Ru(2)	60.1(1)	Ru(1)–Ru(4)–Ru(3)	89.8(1)
Ru(2)–Ru(4)–Ru(3)	51.9(1)	Ru(1)–Ru(4)–B	45.9(4)
Ru(2)–Ru(4)–B	51.4(4)	Ru(3)–Ru(4)–B	44.8(4)
Au–B–Ru(2)	151.9(7)	Rh–B–Ru(4)	160.8(9)
Ru(1)–B–Ru(3)	164.3(9)		

a rocking process, it is possible that in solution the $AuPPh_3$ unit bridges the Rh–B edge rather than capping the Ru(1), Rh, B face as in the solid state; the effect on the nbd protons is the same as in the proposed dynamic process.] Fig. 6(*a*) describes a process that is consistent with the ^1H NMR spectrum at 206 K. At higher temperatures the equivalence of all four olefinic protons and of protons d and e, may be rationalised in terms of the rotation of the nbd ligand, in addition to the motion of the $AuPPh_3$ unit.

A comparison of the IR and NMR spectroscopic data for compounds **3** and **4** with those of **2** suggests that the $P(C_6H_{11})_3$ and $P(C_6H_4Me\text{-}2)_3$ derivatives adopt the same structure as that of cluster **2**; for **3** the signal expected for the CH_2 protons of the nbd ligand is masked by those due to the cyclohexyl ring protons. Since the PR_3 group and the nbd ligand are relatively close in space, the steric demands of the phosphine might be expected to have an effect upon the solution dynamics of compounds **3** and **4**; the Tolman cone angles of PPh_3, $P(C_6H_{11})_3$ and $P(C_6H_4Me\text{-}2)_3$ are 145, 170 and 194°

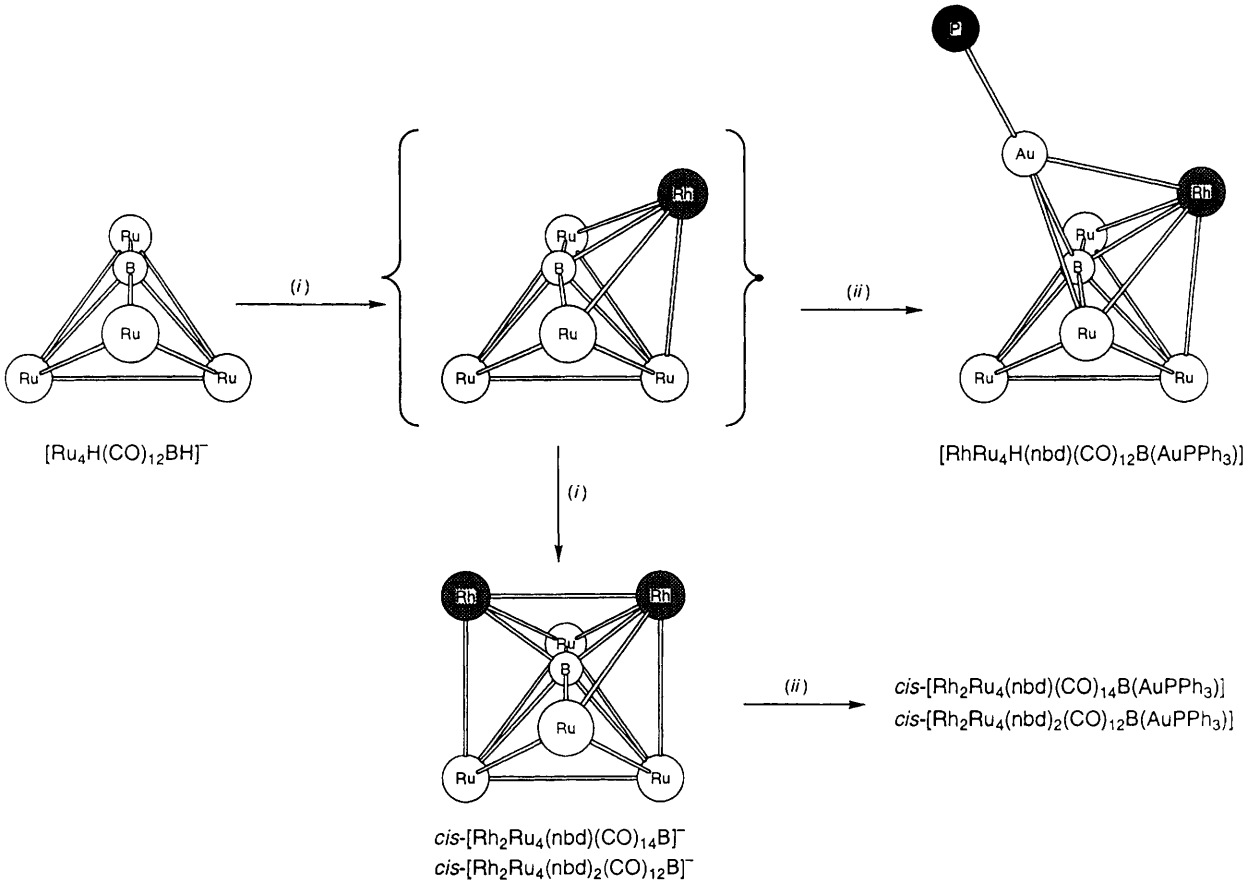

Scheme 2 Proposed route to the formation of compound **2** showing the competitive formation of octahedral Rh_2Ru_4B clusters. (*i*) $[\{Rh(nbd)Cl\}_2]$; (*ii*) $[Au(PPh_3)Cl]$

respectively.[21] Fig. 6(*d*) shows the ^1H NMR spectroscopic resonances for the bridgehead and olefinic protons in cluster **3** at 298 and 181 K. The same pattern as for compound **2** is observed with the significant difference that at room temperature the two resonances are sharp. This would be consistent with a *more* facile rotation of the nbd ligand in compound **3** than in **2**, a result not expected from the trend in the Tolman cone angles. However, it should be noted that solid-state data reveal that 'real' cone angles, particularly for phosphine ligands involving alkyl groups, may vary, and a range of 163–181° for metal-bound $P(C_6H_{11})_3$ has been quoted.[22] The variable-temperature ^1H NMR spectroscopic data for the $P(C_6H_4Me\text{-}2)_3$ derivative **4** are very similar to those of the triphenylphosphine derivative [compare Fig. 6(*e*) with 6(*c*)], although the (very slightly) broader signal assigned to the bridgehead protons in **4** suggests that rotation of the nbd ligand is more hindered in **4** than in **2**, in keeping with the greater steric demands of the $P(C_6H_4Me\text{-}2)_3$ ligand.

A further feature of note in the ^1H NMR spectra of compound **2** is the rather different chemical shifts for the two signals assigned to protons d and e (Fig. 6). Whilst the resonance at δ 3.72 is quite typical of a bridgehead proton in a rhodium-bound nbd ligand,[23] the signal at δ 2.41 is significantly shifted. This is also the case in compound **4**, but for cluster **3** both bridgehead protons appear at similar shifts (δ 3.65 and 3.89). We attribute these differences to the proximity of one bridgehead proton [d in Fig. 6(*b*)] to the aryl rings of the phenyl substituents in **2** or the 2-MeC_6H_4 in **4**.

Reactions of $[RhRu_4H(nbd)(CO)_{12}B(AuPR_3)]$ (R = Ph or C_6H_{11}) with CO

Both compounds **2** and **3** react with CO (50–60 atm) with displacement of the norbornadiene ligand by 2 moles of CO. The spectroscopic data are consistent with there being no change to the cluster core; in particular, there is no shift in the ^{11}B NMR signal. In the ^1H NMR spectra of the two products, signals due to the nbd ligand are absent and for each compound a hydride signal close to δ −18 is observed. These observations along with mass spectral data are consistent with the substitution of nbd by two equivalents of CO. The products are thus formulated as $[RhRu_4H(CO)_{14}B(AuPPh_3)]$ and $[RhRu_4H(CO)_{14}B\{AuP(C_6H_{11})_3\}]$, and we propose structures analogous to that confirmed for **2** (Fig. 4).

Conclusion

We have shown that heterometallic pentametallic boride clusters can be prepared by the addition of a suitable rhodium fragment to the anion $[Ru_4H(CO)_{12}BH]^-$. With $[\{Rh(\eta^5\text{-}C_5Me_5)Cl_2\}_2]$, $[RhRu_4H_2(\eta^5\text{-}C_5Me_5)(\mu\text{-}Cl)(CO)_{12}B]$ is formed in which the five metal atoms adopt an open skeletal structure, but with $[\{Rh(nbd)Cl\}_2]$ the preference is for the formation of octahedral Rh_2Ru_4-based clusters, each containing an interstitial boron atom. However, in this case phosphinegold(I) chlorides can be used to trap a product of the type $[RhRu_4H(nbd)(CO)_{14}B(AuPR_3)]$ containing a square-based pyramidal $RhRu_4$ core.

Acknowledgements

We thank the donors of the Petroleum Research Fund, administered by the American Chemical Society, for support of this work (grant no. 25533-AC3), the SERC for a studentship (to A. D. H.) and the National Science Foundation for a grant (CHE 9007852) towards the purchase of a diffractometer at the University of Delaware.

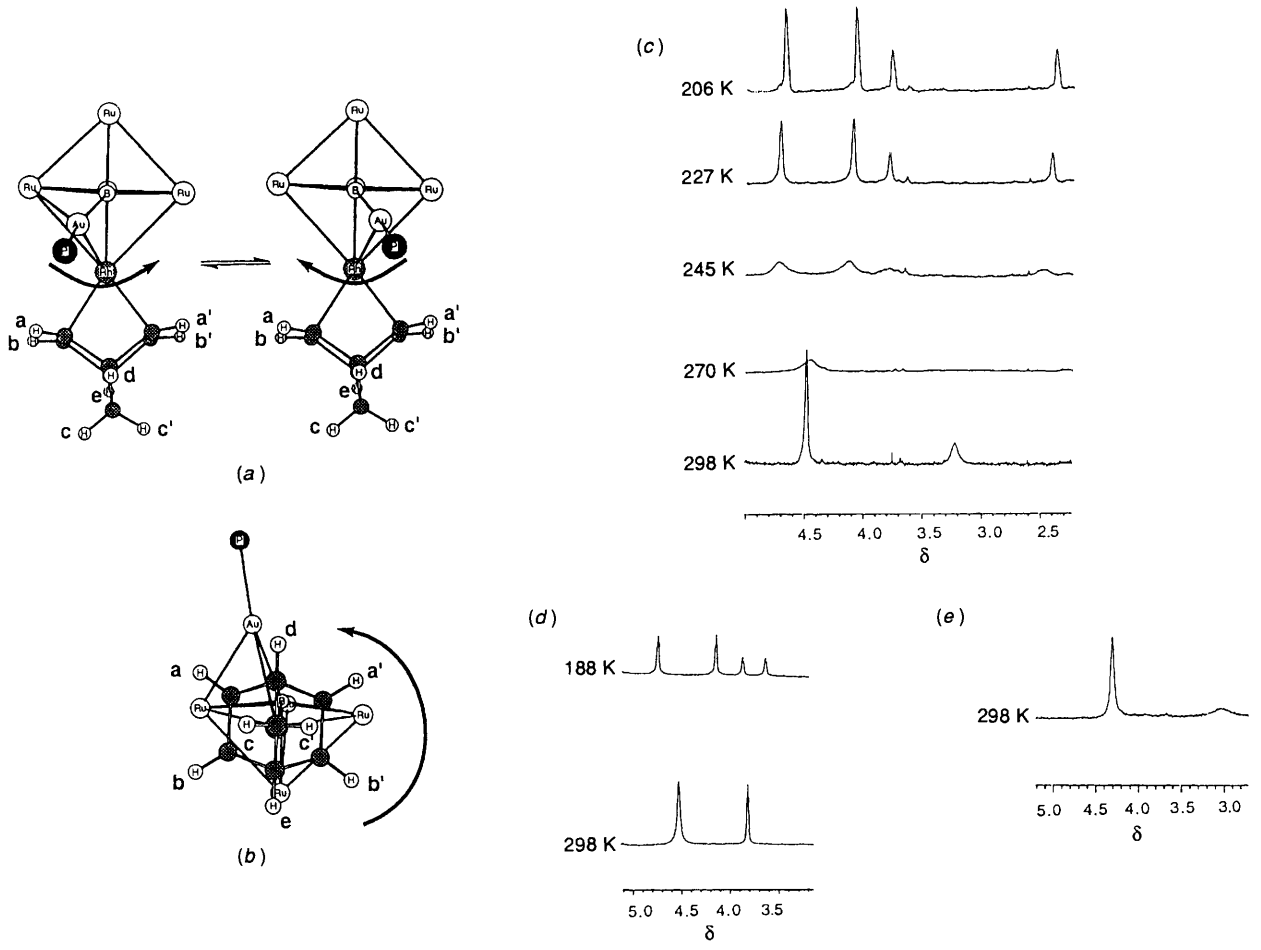

Fig. 6 The two proposed fluxional processes in compounds **2**–**4**: (*a*) the lower-energy rocking of the AuL unit and (*b*) rotation of the nbd ligand. The labelling scheme for the H atoms is common to the two figures. The 400 MHz ^{1}H NMR spectra of **2** (CD_2Cl_2) (*c*), **3** ($CDCl_3$) (*d*) and **4** (CD_2Cl_2) (*e*) in the region showing the olefinic and bridgehead protons of the nbd ligand are also presented

References

1 C. E. Housecroft, *Coord. Chem. Rev.*, 1995, **143**, 297.
2 C. E. Housecroft, *Chem. Soc. Rev.*, 1995, **24**, 215.
3 S. M. Draper, C. E. Housecroft, J. E. Rees, M. S. Shongwe, B. S. Haggerty and A. L. Rheingold, *Organometallics*, 1992, **11**, 2356.
4 C. E. Housecroft, D. M. Matthews and A. L. Rheingold, *Organometallics*, 1992, **11**, 2959.
5 J.-H. Chung, D. Knoeppel, D. McCarthy, A. Columbie and S. G. Shore, *Inorg. Chem.*, 1993, **32**, 3391.
6 C. S. Jun, T. P. Fehlner and A. L. Rheingold, *J. Am. Chem. Soc.*, 1993, **115**, 4393.
7 F. H. Allen, J. E. Davies, J. J. Galloy, O. Johnson, O. Kennard, C. F. Macrae, E. M. Mitchell, G. F. Mitchell, J. M. Smith and D. G. Watson, *J. Chem. Inf. Comput. Sci.*, 1991, **31**, 187.
8 A. K. Chipperfield, C. E. Housecroft and A. L. Rheingold, *Organometallics*, 1990, **9**, 681.
9 F. G. Mann, A. F. Wells and D. J. Purdie, *J. Chem. Soc.*, 1937, 1828; D. R. Williamson and M. C. Baird, *J. Inorg. Nucl. Chem.*, 1972, **34**, 3393; A. N. Nesmeyanov, E. G. Perevalova, Yu. T. Struchkov, M. Yu. Antipin, K. I. Grandberg and V. P. Dyadchenko, *J. Organomet. Chem.*, 1980, **201**, 343.
10 M. I. Bruce and B. K. Nicholson, *J. Organomet. Chem.*, 1983, **252**, 243.
11 A. D. Hattersley, C. E. Housecroft and A. L. Rheingold, paper in preparation.
12 SHELXTL PC software, version 4.2, G. Sheldrick, Siemens XRD, Madison, WI, 1990.
13 J. R. Galsworthy, C. E. Housecroft, A. J. Edwards and P. R. Raithby, *J. Chem. Soc., Dalton Trans.*, 1995, 2935.
14 J. R. Galsworthy, C. E. Housecroft, J. S. Humphrey, X. Song, A. J. Edwards and A. L. Rheingold, *J. Chem. Soc., Dalton Trans.*, 1994, 3273.
15 See, for example, B. F. G. Johnson, J. Lewis, J. M. Mace, P. R. Raithby and M. D. Vargas, *J. Organomet. Chem.*, 1987, **321**, 409; J. A. Cabeza, F. J. Lahoz and A. Martin, *Organometallics*, 1992, **11**, 2754.
16 C. E. Housecroft and S. M. Owen, *Organometallics*, 1988, **7**, 1385.
17 G. Lavigne, F. Papageorgiou and J.-J. Bonnet, *Inorg. Chem.*, 1984, **23**, 609.
18 F.-E. Hong, D. A. McCarthy, J. P. White, C. E. Cottrell and S. G. Shore, *Inorg. Chem.*, 1990, **29**, 2874.
19 J. R. Galsworthy, A. D. Hattersley, C. E. Housecroft, A. L. Rheingold and A. Waller, *J. Chem. Soc., Dalton Trans.*, 1995, 549.
20 R. Khattar, J. Puga, T. P. Fehlner and A. L. Rheingold, *J. Am. Chem. Soc.*, 1989, **111**, 1877; A. K. Bandyopadhyay, R. Khattar and T. P. Fehlner, *Inorg. Chem.*, 1989, **28**, 4434; A. K. Bandyopadhyay, R. Khattar, J. Puga, T. P. Fehlner and A. L. Rheingold, *Inorg. Chem.*, 1992, **31**, 465.
21 C. A. Tolman, *Chem. Rev.*, 1977, **77**, 313.
22 C. A. McAuliffe, in *Comprehensive Coordination Chemistry*, eds. G. Wilkinson, R. D. Gillard and J. A. McCleverty, Pergamon, Oxford, 1987, vol. 2, p. 1023.
23 R. P. Hughes, in *Comprehensive Organometallic Chemistry*, eds. G. Wilkinson, F. G. A. Stone and E. W. Abel, Pergamon, Oxford, 1982, vol. 5, p. 479.

Received 28*th July* 1995; *Paper* 5/06043E